

## THERMAL INVESTIGATION OF BAKING NEAPOLITAN PIZZAS IN INNOVATIVE ELECTRIC OVEN

Mena Ciarmiello, Biagio Morrone<sup>§</sup> and Fulvio Trasacco

Department of Industrial and Information Technology Engineering, University of Campania

"Luigi Vanvitelli", Aversa, Italy

<sup>§</sup>Correspondence author. Fax: +39 081 5010204 Email: biagio.morrone@unicampania.it

**ABSTRACT** *True* Neapolitan pizza should be baked in traditional wood-fired ovens, according to Specification of Production n°56/2010. However, airborne and hazard pollutants due to wood combustion may lead to severe air quality impacts, so that design and development of electric oven, alternative to wood-fired ones, is a suitable target for air pollution control strategies.

In this paper a three-dimensional Computational Fluid Dynamic (CFD) model has used to evaluate thermal performances of an electric oven for Neapolitan pizzas. The CFD model comprises the continuity, momentum and energy equations, whereas the standard  $k-\varepsilon$  approach has been used for turbulence closure and *surface-to-surface* model has been applied for radiation. Coupled conduction-convection and radiation is taken into account to assess the walls that bound the cooking chamber. Electric heaters located into the bed and dome walls of the cooking chamber provide the heat generation, allowing the baking of pizzas.

A condition of full load oven has considered, consisting of nine pizzas placed on the bed of the cooking chamber and different thermo-physical model properties have been investigated, with a baking time of 90 s. Results have highlighted that the radiative heat transfer is the predominant mechanisms for pizza baking. Moreover, the role of pizza emissivity on temperature time evolution has been investigated, considering three different emissivity values. In addition, results have been compared with a model with constant thermo-physical properties for pizza, scrutinizing the role of such parameters on thermal baking performance.

## INTRODUCTION

*True* Neapolitan pizza is a traditionally cooked in wood-fired ovens, according to strict Specification of Production, so that the Traditional Specialty Guaranteed (TSG) quality is awarded by Commission Regulation (EU) n°97/2010.

Nevertheless, in recent years, it has been widely recognized that the use of solid fuels for cooking operations, such as biomass and coal, contributes to elevated concentrations of hazardous pollutants [Oluwole et al. 2013; Shen et al. 2014; Alves et al. 2015]. Stack emission generated by biomass particle combustion is a rather complex matter, due to many sub-processes involved and undesirable by-products [Porteiro et al. 2006].

Airborne particles smaller than 2.5  $\mu\text{m}$  ( $\text{PM}_{2.5}$ ), as polycyclic aromatic hydrocarbons (PAHs), dioxins and furans are generally products of combustion, depending on completeness of combustion [Beauchemin and Tampier 2008]. Further, emissions from burning or combustion of biomass are characterized by higher organic carbon and particle emission rates compared to high efficiency fossil fuel combustion sources [Lewtas 1985; Lewtas 2007].

As a consequence, two fundamental objectives should be provided: on the one hand, the air pollution prevention strategies, on the other hand the preserving Neapolitan pizza as excellence in Italian cooking tradition.

For these reasons, the development of an electric oven specifically designed for Neapolitan pizza alternative to traditional wood-fired ovens is a proper objective.

In a previous paper, Ciarmiello and Morrone [2016a] developed a three-dimensional numerical model for an electric oven specially designed for Neapolitan pizza cooking, analysing thermal conditions when the oven was empty. In a further study, Ciarmiello and Morrone [2016b] included nine pizzas placed in the cooking chamber, i.e. a full-load oven condition, and modelled pizzas as solids with constant thermo-physical properties.

However, during the cooking process, physical and chemical changes of dough occur, produced by simultaneous heat and mass transfer. To best knowledge of the authors, no literature focused on pizza baking processes. Purlis [2012] developed a theoretical approach for optimal design of the bread baking process, based on starch gelatinization mechanism and modelling thermo-physical properties depending on temperature and moisture content.

In this paper, a three-dimensional CFD numerical model of the same electric oven for pizzas is presented and discussed, including the thermo-physical properties variability of pizzas and analyzing the effects of temperature on thermal conditions. The model is based on finite volume method (FVM). Pizzas have been modeled as solid and homogeneous materials with constant density; moisture content and evaporation of water in dough have not been taken into account directly, but by means of variability of pizza thermo-physical properties with temperature, as defined in Purlis [2012].

As in the previous works, the geometry and the operating conditions used for this study are obtained by manufacture's documentation.

In the end, in order to consider the uncertainty of some modeling parameters, such as thermal emissivity of the pizzas, an evaluation of thermal cooking performance is considered.

## NOMENCLATURE

A	surface area, m <sup>2</sup>
c	solid specific heat, J kg <sup>-1</sup> K <sup>-1</sup>
c <sub>p</sub>	fluid specific heat, J kg <sup>-1</sup> K <sup>-1</sup>
E	emissive power, W m <sup>-2</sup>
e <sub>gen</sub>	energy source term, W
F <sub>ij</sub>	view factor, -
g	gravitational acceleration, m s <sup>-2</sup>
J	radiosity, W m <sup>-2</sup>
p	pressure, Pa
Q	thermal power, W
q	heat flux, W m <sup>-2</sup>
r	vector position, m
t	time, s
T	temperature, K
T <sub>f</sub>	change of phase temperature, K
V	velocity vector, m s <sup>-1</sup>
W	Moisture content of pizza –

## Greek symbols

δ	Dirac delta function
ε	emissivity, -
λ	thermal conductivity, W m <sup>-1</sup> K <sup>-1</sup>
λ <sub>v</sub>	latent heat during phase change, J kg <sup>-1</sup>
ρ	density, kg m <sup>-3</sup>
τ	stress tensor, Pa

## Subscripts

conv	convective
eff	effective
p	large enclosure wall
pizza	pizza
rad	radiative
w	external wall
wall	cooking chamber wall
0, $\infty$	operating and external condition

## MODELLING METHODS

### Physical Model

The electric oven consists of three parts: the cooking chamber, where pizzas are baked, and the inner and outer wall layers, made of refractory bricks and rock wool, respectively, reported in Figure 1. Walls are designed to reduce as much as possible the heat transfer from the oven to the environment. The external oven sizes, are equal to 1.53 m in length, 1.63 m in depth and 0.64 m in height, respectively.

The cooking chamber has a rectangular cross-section of 1.03 m in length and 1.13 m in width. Pizzas are put into the oven through the open section located on the front, with a maximum oven load of nine pizzas. Pizzas have been modelled as a homogenous solid material, with a diameter of 33 cm and a uniform thickness of 1.2 cm; the properties of pizzas are detailed in the *Material Properties* section.

Heat generation is provided by two nickel-alloy electrical heaters, embedded in the bed and dome of refractory bricks delimiting the cooking chamber. The dome electric heater has a power of 11.2 kW, while the resistance of the bed has a power of 3.4 kW, according to manufacturer's specifications. The external ambient and the initial pizza temperatures are set to 298 K.

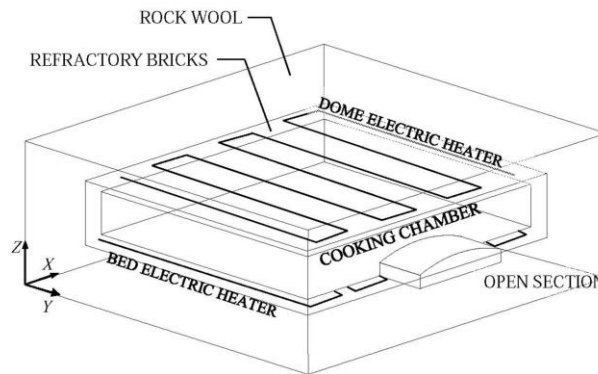


Figure 1 Sketch of the oven in an axonometric schematic view.

### Governing Equations

The control volume includes the air volume of the cooking chamber as well as the solid walls made of refractory bricks and rock wool layers.

The continuity and momentum equations for the three-dimensional Cartesian coordinates in the fluid domain (using the notation of the substantial derivative) are:

$$\frac{\partial \rho}{\partial t} + \nabla \cdot (\rho \mathbf{V}) = 0 \quad (1)$$

$$\rho \frac{D\mathbf{V}}{Dt} = -\nabla p + \rho \mathbf{g} + \nabla \cdot \boldsymbol{\tau} \quad (2)$$

The mass force term in Eq.(2) has been linearized using the Boussinesq approximation. The last term on the right side of Eq.(2) is the stress tensor, which consists of viscosity for Newtonian fluid and turbulent components. Turbulence closure of momentum and energy equations has been performed using a standard  $k-\varepsilon$  model. Because of the energy coupling between fluid and solid regions, energy equations are considered both for fluid and solid subdomains:

- *fluid domain*

$$\frac{\partial}{\partial t} \rho c_p T + \nabla \cdot (\mathbf{V} \rho c_p T) = \nabla \cdot (\lambda_{eff} \nabla T) \quad (3)$$

- *solid domains*

$$\frac{\partial (\rho c T)}{\partial t} = \nabla \cdot (\lambda \nabla T) + e_{gen} \quad (4)$$

Eq.(4) applies to both solid subdomains: one in which the heat generation is supplied by electric heaters through bed and dome walls and solid walls which bound the cooking chamber (Figure 1) and where heat source is not provided, thus having  $e_{gen}=0$ .

The imposed thermal boundary conditions on walls facing external environment are mixed heat flux condition:  $q_w = q_{conv} + q_{rad}$  with  $q_{conv}$  the convective and  $q_{rad}$  the radiative terms. The heat transfer coefficient between the external walls and environment has been set equal to  $8 \text{ W m}^{-2}\text{K}^{-1}$ , the emissivity of external walls  $\varepsilon_w = 1.0$ , and the environment temperatures set equal to 298 K. The open flow section is an open boundary with assigned discharge coefficient, set to 0.3, so that the airflow is allowed flowing inward or outward the cooking chamber. Electric heaters for heat generation undergo an *on/off cycle* depending on the bed and dome average temperatures. The threshold for switching from *on* to *off* condition has been set to 758 K, with a  $\pm 2\text{K}$  band.

Radiation model: The *surface-to-surface* radiation model has been used, considering a perfectly transparent fluid medium and grey and diffuse surfaces. The total energy given off by each surface  $i$ , i.e. the radiosity  $J_i$ , is obtained by the energy emitted by the surface and the reflected energy coming from other surfaces, according to the following equation:

$$J_i = E_i + (1 - \varepsilon_i) \sum_j^N F_{ji} J_j \quad (5)$$

with  $F_{ji}$  the view factors, which represents the fraction of energy leaving the  $i$ -th surface and directly hitting the  $j$  surface and  $\varepsilon_i$  the emissivity of  $i$  surface.

**Material Properties** Materials properties were defined for the walls of the cooking chamber, and pizzas, considering isotropic and homogeneous solids. Table 1 shows the thermo-physical properties of the walls, both for the refractory bricks and rock wool layer, as reported in Ciarmiello and Morrone [2016b].

Pizzas have been modelled as discs of homogeneous solid material with constant density and thickness. Temperature dependence for thermal conductivity and specific heat was considered according to Purlis

[2012], as shown in Table 2, whereas mass transfer processes were neglected. The enthalpy jump is simulated by the Delta-type function  $\delta(T-T_f, \Delta T)$ , being  $T_f=373$  K (100°C) the temperature of phase change and  $\Delta T=0.5^\circ\text{C}$  the temperature range of phase change.

Table 1  
Thermo-physical properties of cooking chamber walls.

	$\rho$ ( $\text{kg m}^{-3}$ )	$\lambda$ ( $\text{W m}^{-1} \text{K}^{-1}$ )	$c$ ( $\text{J kg}^{-1} \text{K}^{-1}$ )
Refractory bricks	1850	$0.564+0.0007 T[\text{K}]$	1050
Rock wool	50	0.04	840

Since the specific heat is affected by the moisture content of dough, determination of this quantity has been experimentally obtained. Moisture of dough, indicated by  $W$  in the next equations, has been scrutinized equal to  $26.6\% \pm 4.2$ , using six replicates. The procedure to assess the moisture of dough has been obtained following the standard [AACC 44-01.01 1999].

In addition, a constant thermo-physical properties model has been taken into account, as defined in Ciarmiello and Morrone [2016b].

Table 2  
Thermo-physical properties of pizzas.

$\rho_{pizza}$ ( $\text{kg/m}^3$ )	$\lambda_{pizza}$ [Purlis 2012] ( $\text{W m}^{-1} \text{K}^{-1}$ )	$c_{p,pizza}$ [Purlis 2012] ( $\text{J kg}^{-1} \text{K}^{-1}$ )
790	$\lambda(T) = 0.9 / \{1 + \exp[-0.1(T - 353.16)]\} + 0.2$  $\lambda(T) = 0.2$	$c_p(T, W) = c_p^*(T, W) + \lambda_v W \delta(T - T_f, \Delta T)$  $c_p^*(T, W) = c_{p,s}(T) + W c_{p,w}(T)$  $c_{p,s}(T) = 5T + 25$  $c_{p,w}(T) = 5207 - 7.317T + 1.35 \times 10^{-2} T^2$

**Simulated Conditions** Numerical simulations have been carried out both for constant and temperature-dependent thermo-physical conditions (Table 2) for three pizza emissivity values, as reported in the following Table 3. After steady state was achieved with bed and dome electric heaters set to *on* condition [Ciarmiello and Morrone 2016b], nine pizzas (*full-load oven*) at initial temperature of 298 K were placed on the bed of the cooking chamber, meanwhile the electric heaters were set to *on/off* cycle during the overall cooking time, that lasts 90 s, and considering a perfect contact between lower pizza surface and the bed surface.

Table 3  
Thermo-physical properties of the pizzas.

Constant thermo-physical properties	Temperature dependent thermo-physical properties
$\varepsilon=1.0$	$\varepsilon=1.0$
$\varepsilon=0.85$	$\varepsilon=0.85$
$\varepsilon=0.60$	$\varepsilon=0.60$

## RESULTS AND DISCUSSION

### Numerical Model and Validation

In Figure 2 the positioning of the nine pizzas into the oven, referred to the front opening is reported. In the same figure, the locations of the points inside pizzas employed for the numerical validation, are also included.

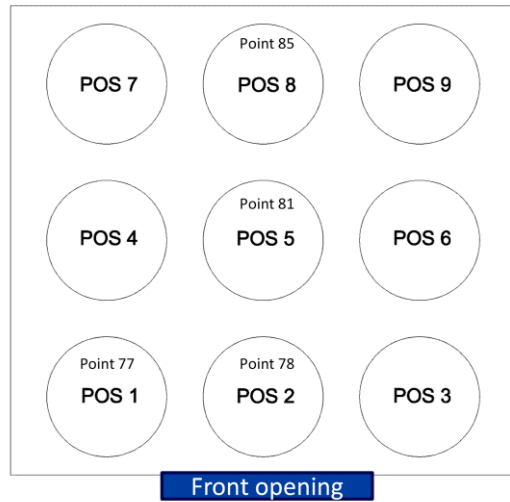


Figure 2 Placement of pizzas with position number and location of points inside the oven.

The numerical validation has been obtained by comparing the solutions with different time steps and different cell nodes of the grid. In Table 4 the mesh cells employed in the assessment of numerical procedure validation are reported. The three meshes are indicated as *Mesh 1*, *Mesh 2* and *Mesh 3* and the corresponding total cell numbers are reported in the same table.

Figure 3 shows temperature distribution at different locations, indicated with *point 77*, *point 78*, *point 81* and *point 85* as a function of the time with four different time steps (0.1 s, 0.2 s, 0.5 and 1.0 s) using *Mesh 2*. An extremely good agreement among the numerical results is observed for all the investigated time steps, except when  $\Delta t$  is equal to 1.0 s, with the numerical solutions showing smaller temperature values (green triangle) starting from about 60 s. Anyway, the percent difference is smaller than 1% between the solution with the largest and smallest  $\Delta t$ . Considering that the temperature distributions show negligible differences in the next results are presented with a  $\Delta t = 0.5$  s.

Table 4  
Number of cells for distinct grid mesh employed.

	Cells
<i>Mesh 1</i>	171,427
<i>Mesh 2</i>	344,785
<i>Mesh 3</i>	806,209

The comparison among the three mesh grids is reported in Figure 4, for the Total (THF) and the Radiative Heat Fluxes (RHF) of the dome, at the end of the cooking time of pizzas in the oven (i.e. after 90 s). Small differences between the *Mesh 2* and *Mesh 3* are observed, with a percentage of about 6%.

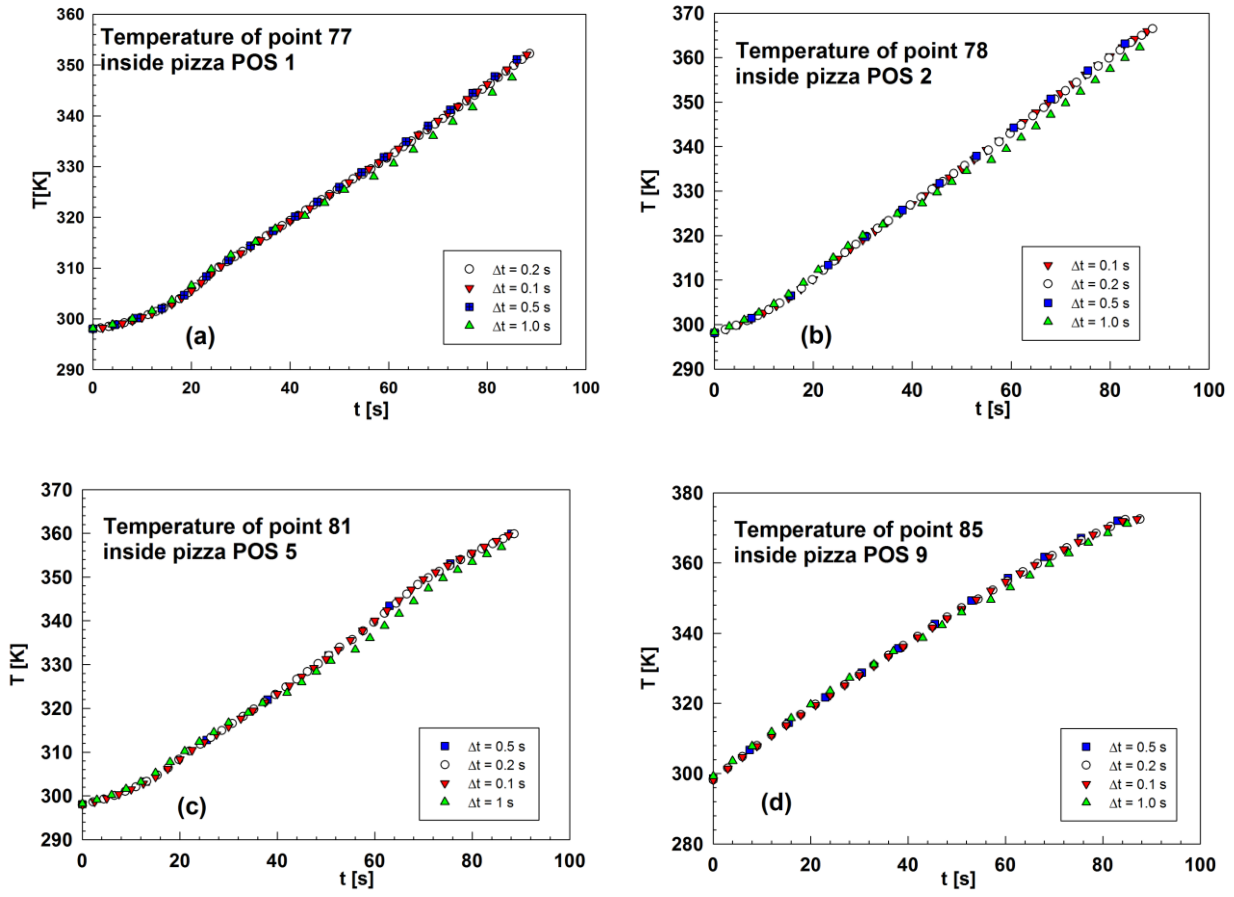


Figure 3 Comparison of temperature distribution for different  $\Delta t$  and at different locations: (a) point 77 POS 1, (b) point 78 POS 2, (c) point 81 POS 5, (d) point 85 POS 8.

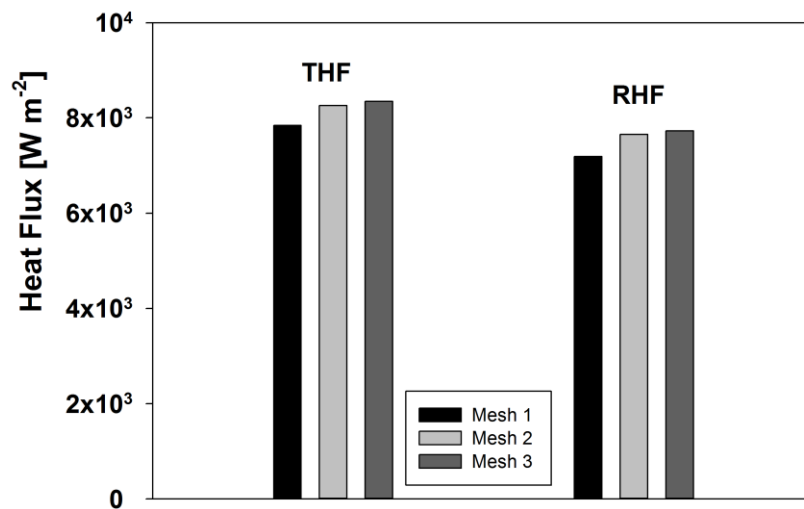


Figure 4 Comparison of dome THF and RHF among the three diverse investigated meshes

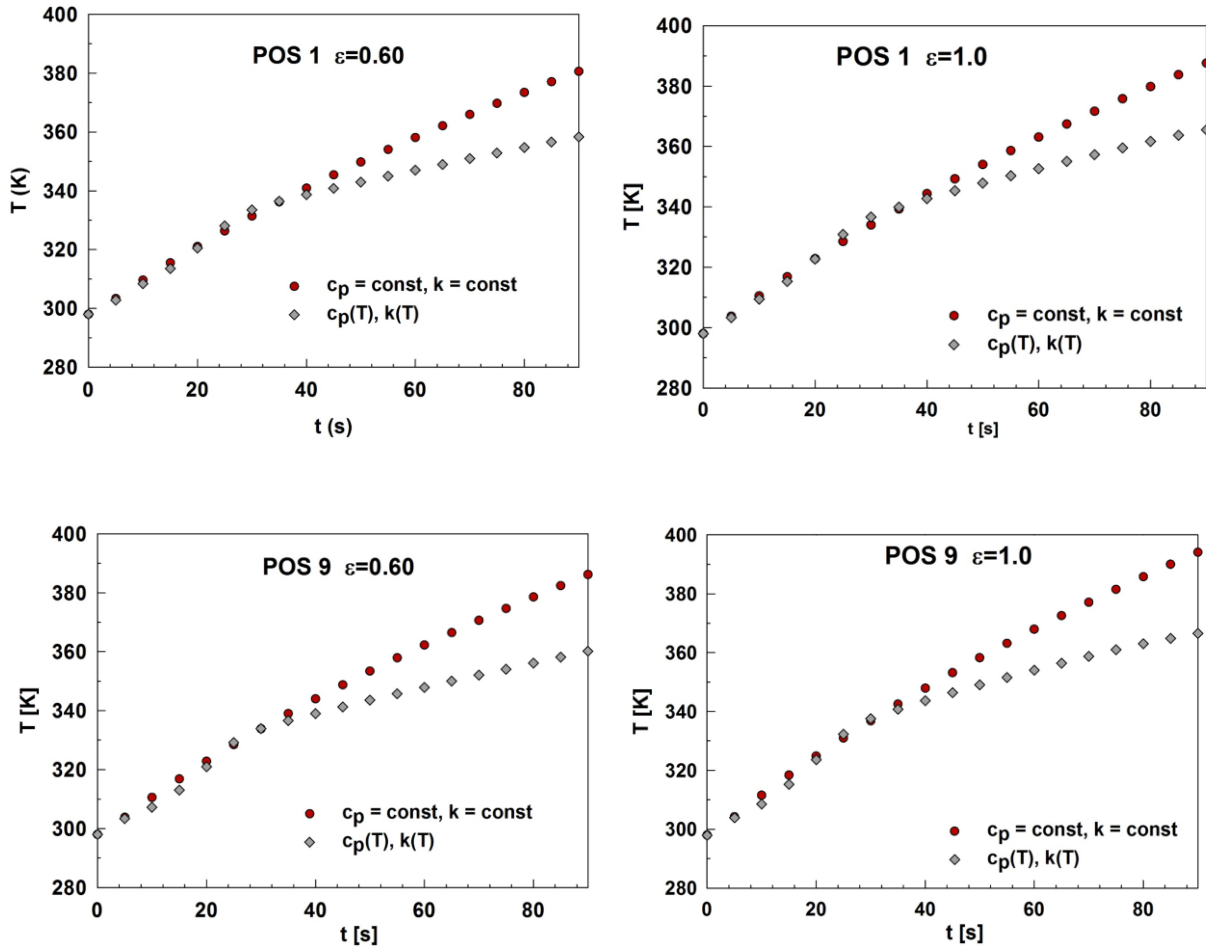


Figure 5. Comparison of calculated volume-averaged pizza temperatures as a function of time between constant and variable thermo-physical properties models at different positions of pizza in the cooking chamber with pizza emissivity  $\varepsilon=0.60$  and  $\varepsilon=1.0$ .

Other comparisons, not shown in this paper, present the same trend. Thus, the results presented in the following have been obtained using *Mesh 2* and a  $\Delta t = 0.5$  s.

The next comparison is between the constant properties model and temperature-dependant one, to assess the impact of model on the results.

The comparison of time evolution of volume-averaged pizza temperatures located at POS 1 and POS 9 (see Figure 2) is reported in Figure 5. Pizza emissivity has been set to  $\varepsilon=0.60$  and  $\varepsilon=1.0$ .

It can be observed that both temperatures show the same trend. For the POS 1 location, both the emissivity values show that the variable thermal properties model has lower temperatures attaining a maximum of about 360 K, whereas the constant properties model has larger temperatures, starting from about 40 s. This is due to the specific heat function of temperature which accounts for the moisture evaporation in the dough, limiting the temperature increase. Similar considerations can be acquired from pizza located at POS 9, anyway even larger temperature values are observed in this case. As a general remark, larger emissivity value results in higher temperature discrepancies between the two models.

The Radiative Heat Flux (RHF) from the dome is reported in Figure 6 for the two emissivity values,  $\varepsilon=0.60$  and  $\varepsilon=1.0$  comparing the two models. In the first part of time evolution, until 70 s, the constant properties model presents higher RHF, both Figure 6(a) and Figure 6(b), than variable properties model. This can be due to the higher average temperatures shown by the constant properties model.

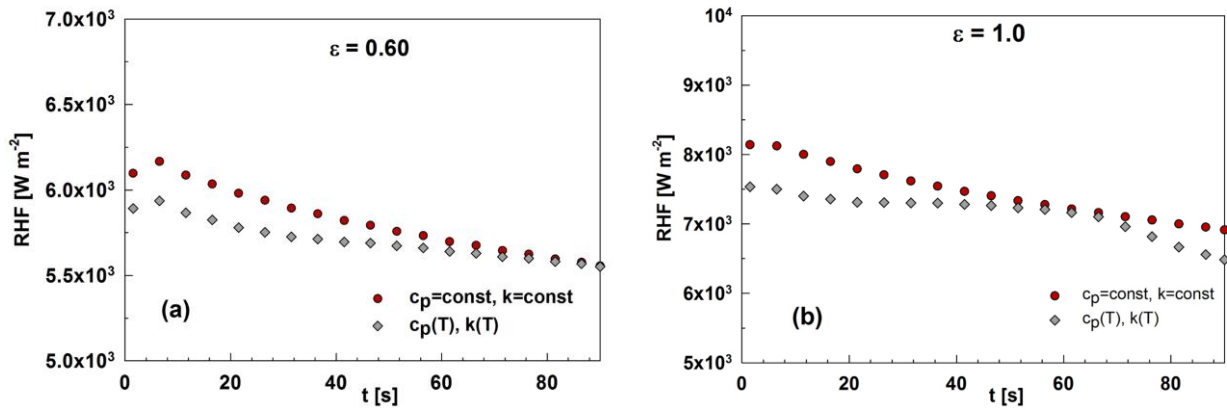


Figure 6 Radiative Heat Flux (RHF) on the dome for two emissivity values, constant and temperature-dependent properties.

Once assessed the difference between the two property models (constant and variable) and considering from now on the variable properties model, the following investigations focus on the different thermal behaviours when discrepant emissivity values are taken into account.

The surface average temperature-time evolutions are reported in Figure 7(a) for the dome and Figure 7(b) for the bed of the cooking chamber with three different emissivity values. It is evident that the dome temperature is largely affected by the emissivity of pizzas. In fact, the larger the emissivity is the lower the dome temperature. This is due to the constant power heating released by the electric heater and the larger amount of radiative heat absorbed by pizzas with  $\epsilon=1.0$ , thus implying a reduction of the average wall temperature of the dome. Instead, when focusing on the lower wall, i.e. the bed, of the cooking chamber, no appreciable temperature-time evolution differences can be detected since the heat transfer between the floor and the pizzas is quite completely by conduction. Thus, the decrease of average bed temperature (Figure 7(b)) during the first phase of baking process is due to the perfect contact between a very hot surface and a solid (pizza) surface whose temperature is at the beginning of the process equal to the environment, i.e. 298 K.

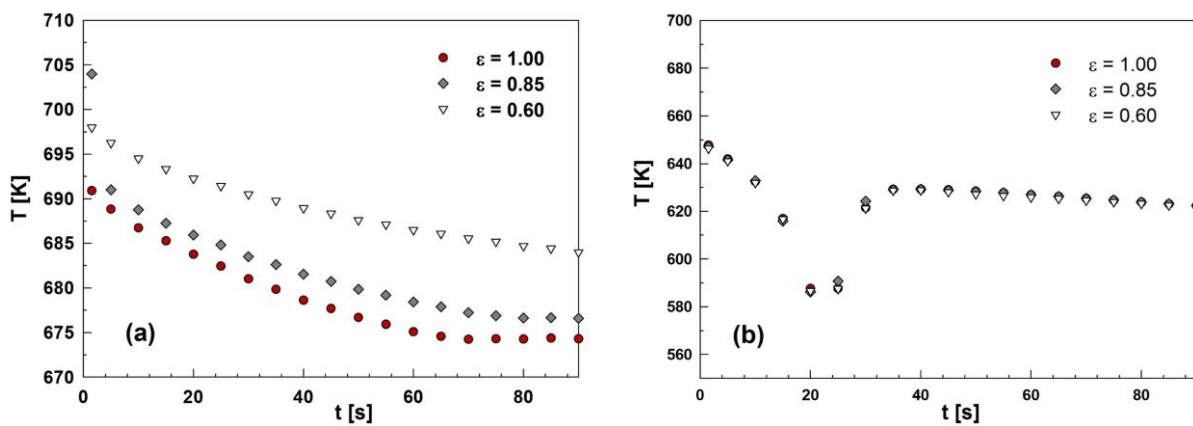


Figure 7 Average temperature distribution as a function of the time on the (a) dome and (b) bed of the cooking chamber.

Average temperature-time evolutions for four positions of pizzas (POS 1, 2, 5 and 9) and different emissivity values are reported in Figure 8. The main observed trend is that the smaller the emissivity of pizzas the lower the average temperature, after about 30 s from the starting of baking process. Anyway also discrepancies are observed. In fact, the two pizzas located in the first row as regards the open section show a smooth increment of temperature with a slowing down when temperature attains about 340 K (i.e. after about 30 s). Instead, pizza located in POS 9 shows a different trend. In fact, nearly a stepwise variation occurs at about 20 s increasing temperature value of about 10 K. In addition, no significant differences can be observed between solid with emissivity  $\varepsilon = 1.0$  and 0.85, since pizza is not exposed to the outside environment, which instead happens for solids located at POS 1 and POS 2. These two positions are more exposed to the environment and thus to the radiative heat transfer towards the environment, resulting in temperature discrepancies between pizzas with different emissivity values. Smaller temperature differences are observed at POS 5.

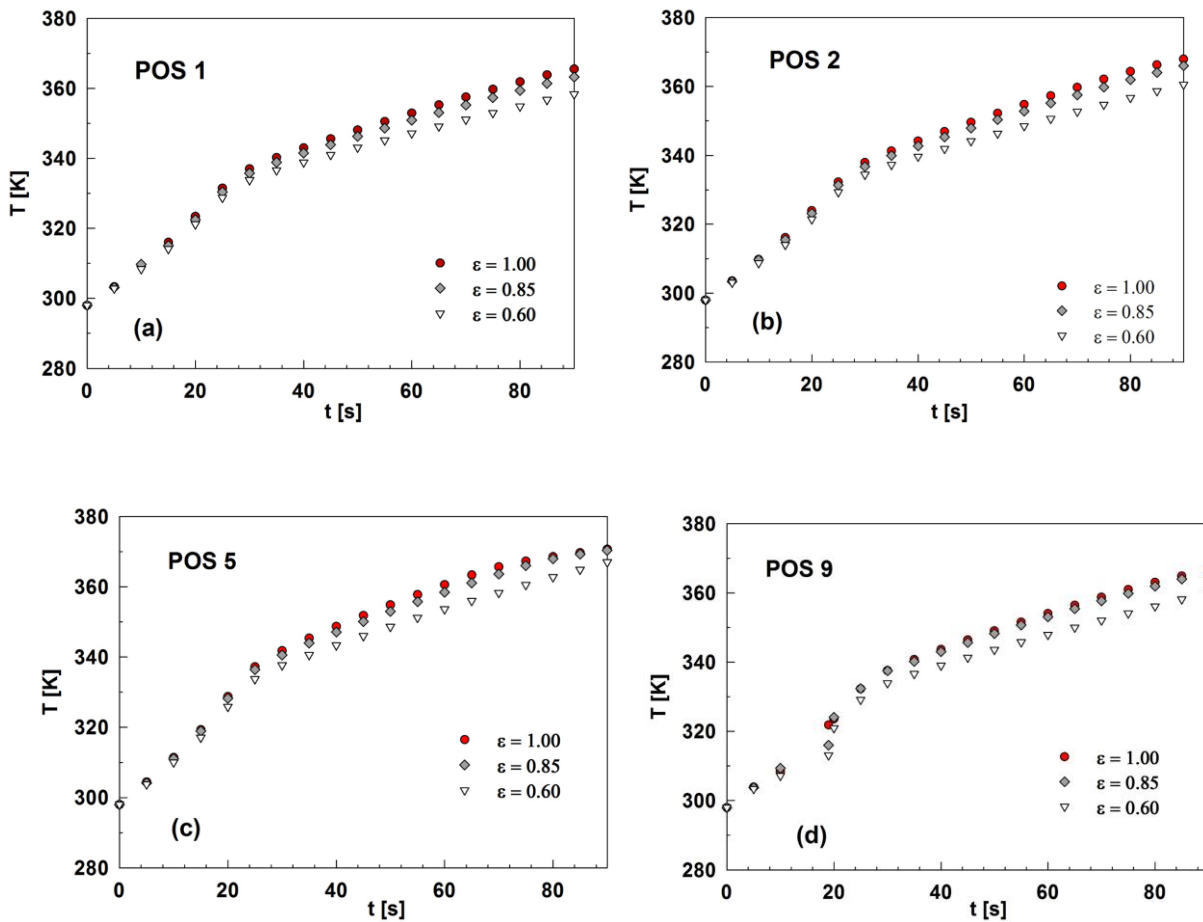


Figure 8. Average pizza temperatures as a function of time with diverse pizza emissivity values, at different positions: (a) POS 1, (b) POS 2, (c) POS 5, (d) POS 9.

Figure 9(a) shows the Total Heat Flux (THF) and Figure 9(b) the Radiative Heat Flux (RHF) as a function of time, on the dome of the baking chamber as a function of time for different values of pizza emissivity values. The main observation is related to the ratio between the RHF and THF, which is always nearly equal to 1. This means that convective heat transfer is almost negligible for this kind of systems. THF behaviour shows nearly a constant value for all the three emissivity values of pizzas, with a larger decrease for higher emissivity value since the temperature of pizzas is larger compared with other emissivity values. Instead, RHF, Figure 9(b), always decreases in the considered time

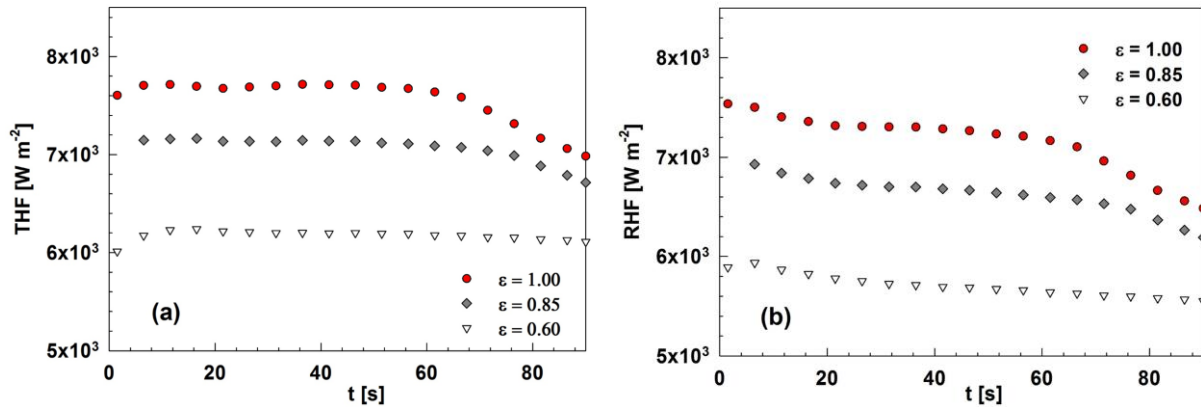


Figure 9. (a) Total Heat Flux, THF and (b) Radiative Heat Flux, RHF on the dome of the baking chamber as a function of the time.

interval because of the increment of pizza temperature and limitation to the electric resistance temperature values.

## CONCLUSIONS

Optimal design of electric oven for Neapolitan pizza is a rather complex challenge due both to many operating variables and thermo-physical properties of the products involved.

In this paper, thermal performances of an innovative electric oven for Neapolitan pizza has been studied, focusing on the role played by the thermo-physical properties of pizzas. Radiation has been recognized to be the predominant heat transfer mechanism. Further, the comparison between the constant properties and temperature-dependant model has shown that lower temperatures of pizzas are attained when the thermo-physical properties of pizzas changes with temperature. As far as the pizza emissivity role, it has been shown that the dome of the cooking chamber is mainly affected by the pizza emissivity variations, whereas no significant temperature modifications occur on bed due to pizza emissivity.

## REFERENCES

- AACC International Method, #44-01.01, [1999], Calculation of Percent Moisture.
- Alves, C.A., Evtugina, M., Cerqueira, M., Nunes, T., Duarte, M. and Vicente, E. [2015], Volatile organic compounds emitted by the stacks of restaurants, *Air Qual Atmos Health*, Vol.8, No. 4, pp. 401-412.
- Beauchemin, P. and Tampier, M. [2008], Emissions from wood-fired combustion equipment, *Report for the Ministry of Environment*, British Columbia, Canada.
- Ciarmiello, M. and Morrone, B. [2016a], Numerical thermal analysis of an electric oven for Neapolitan pizzas. *H&TECH*, Vol.34, Special Issue 2, pp. S351-S358.
- Ciarmiello, M. and Morrone, B. [2016b], Why not Using Electric Ovens for Neapolitan Pizzas? A Thermal Analysis of a High Temperature Electric Pizza Oven, *Energy Procedia*, Vol.101, pp. 1010-1017.

Lewtas, J. [2007], Air pollution combustion emissions: Characterization of causative agents and mechanisms associated with cancer, reproductive, and cardiovascular effects, *Mutation Research/Reviews in Mutation Research* Vol.636, No. 1–3 pp. 95-133.

Lewtas, J. [1985], Combustion emissions: characterization and comparison of their mutagenic and carcinogenic activity. In: H. F. Stich ed., *Carcinogens and Mutagens in the Environment*, CRC Press Boca Raton, FL, pp. 59-74.

Oluwole, O., Ana, G.R., Arinola, G.O., Wiskel, T., Falusi, A.G., Huo, D., Olopade, O.I. and Olopade, C.O. [2013], Effect of stove intervention on household air pollution and the respiratory health of women and children in rural Nigeria, *Air Qual Atmos Health*, Vol.6, No. 3, pp. 553-561.

Porteiro, J., Míguez, J.L., Granada, E. and Moran, J.C. [2006], Mathematical modelling of the combustion of a single wood particle, *Fuel Process Technol*, Vol.87, No. 2, pp. 169-175.

Purlis, E. [2012], Baking process design based on modelling and simulation: Towards optimization of bread baking, *Food Control*, Vol.27, No. 1, pp. 45-52.

Shen, G., Zhang, Y., Wei, S., Chen, Y., Yang, C., Lin, P., Xie, H., Xue, M., Wang, X. and Tao, S. [2014], Indoor/outdoor pollution level and personal inhalation exposure of polycyclic aromatic hydrocarbons through biomass fuelled cooking, *Air Qual Atmos Health*, Vol.7, No. 4, pp. 449-458.